Hindawi
Wireless Communications and Mobile Computing
Volume 2018, Article ID 5391245, 10 pages
https://doi.org/10.1155/2018/5391245

Research Article

Single-Layer, Dual-Port, Dual-Band, and Orthogonal-Circularly Polarized Microstrip Antenna Array with Low Frequency Ratio

Min Wang, Dao-Yu Wang, Wen Wu, and Da-Gang Fang

Ministerial Key Laboratory of JGMT, School of Electronic and Optical Engineering, Nanjing University of Science and Technology, Nanjing 210094, China

Correspondence should be addressed to Min Wang; wangmin@njust.edu.cn

Received 14 December 2017; Accepted 11 March 2018; Published 11 April 2018

Academic Editor: Shichang Chen

A single-layer, dual-port, dual-band, and dual circularly polarized (CP) microstrip array is designed for satellite communication in this paper. The operating frequencies are 8.2 and 8.6 GHz with a very low ratio of 1.05. First, a rectangular patch element is fed through microstrip lines at two orthogonal edges to excite two orthogonal dominant modes of TM_{01} and TM_{10}. The very low frequency ratio can be realized with high polarization isolations. Then, a 2-by-2 dual-band dual-CP subarray is constructed by two independent sets of sequentially rotated (SR) feed structures. An 8-by-8 array is designed on the single-layer thin substrate. Finally, by utilizing one-to-four power dividers and semirigid coaxial cables, a 16-by-16 array is developed to achieve higher gain. Measured results show that the 16-by-16 array has 15 dB return loss (RL) bandwidths of 4.81% and 6.75% and 3 dB axial ratio (AR) bandwidths of 2.84% and 1.57% in the lower and the upper bands, respectively. Isolations of 18.6 dB and 19.4 dB and peak gains of 25.1 dBic and 25.6 dBic are obtained at 8.2 and 8.6 GHz, respectively.

1. Introduction

In satellite communication systems, dual-band antennas are usually required for the uplink and downlink operating at different frequencies. Orthogonal polarization is much preferable to improve the isolation of separate transmit-receive channels, especially for dual-band antennas with a low frequency ratio. Circular polarization is the better choice than linear polarization because of the advantages of insensitivity to antenna orientations, elimination of the signal Faraday rotation effect caused by the ionosphere, and resistance to bad weather conditions. Various antenna types can be used to address the shared-aperture dual-band dual-circular polarized (CP) problems. Planar antennas, such as printed dipoles, slots and microstrip patches, become more favorite candidates attributing to their low profiles.

Traditionally, dual-band dual-linear or circular polarized antennas tend to adopt a multilayer and stacked-patch structure [1–5]. Separate elements are placed on different layers to achieve a dual-band dual-polarized design flexibly. Thus, appropriate frequency ratios can be easily realized [1, 2]. Agile feed networks are designed to form larger arrays with high gain and efficiency [3, 4], improved frequency response [2], and wide bandwidth [5]. The only drawback is that the fabrication process of multilayer antennas is rather difficult and costly.

Several single-layer antenna elements have been proposed to achieve a dual-band and dual-CP radiation. Cross slots with unequal arm-lengths can be loaded on patch antenna [6] or annular-slot [7, 8] to achieve dual-band and dual-CP antennas with a single-layer configuration. Nevertheless, the bidirectional radiation property of these slot antennas limits their applications for satellite. In this context, a dual-band CP planar monopole antenna is presented in [9] by combining an "L"-shaped strip and a "C"-shaped strip. Besides, a circular patch with eight curved slots and a disk-loaded coaxial probe is presented to achieve the dual-band dual circularly polarized pattern [10]. Yet, their omnidirectional radiation is not desirable. It should be pointed out that there is also a single-layer design that can achieve dual-band and dual-CP directional pattern [11]. However, the gain of above-mentioned antennas is relatively low. Moreover, their coaxial probe feeding scheme increases

the difficulty to form a larger array that is much desirable in satellite communications.

Only a few works have been carried out on dual-band dual-polarized antenna arrays with a single-layer substrate [12–14]. In [12], two disparate patches are connected directly to construct a dual-band orthogonal-CP element fed by microstrip line, which can be extended to a larger array easily. A square patch loaded by four stubs is proposed in [13], where two pairs of orthogonal modes, that is, the TM_{10}/TM_{01} and TM_{30}/TM_{03}, are excited simultaneously. In these two cases, the dual-band orthogonal-CP microstrip array has been implemented on a single-layer substrate, but the low frequency ratio is difficult to achieve. The realized ratios of two center frequencies are 1.44 and 1.42, respectively, which are rather high for some particular satellite communication applications. In [14], a low frequency ratio of 1.14 is achieved by exciting TM_{10} and TM_{01} modes of a rectangular patch, while it is orthogonal linear polarized (LP). In addition, these configurations tend to have only a single port, which is not suitable for systems with separate transmit-receive antennas.

In this paper, a dual-port, dual-band, and dual-CP microstrip array on a single-layer substrate is presented. First, by exciting two orthogonal dominant modes of TM_{01} and TM_{10}, a rectangular patch is adopted to realize a very low frequency ratio, while radiating the orthogonal-LP waves. For a specific satellite communication system, the element is designed at 8.2 GHz and 8.6 GHz with a ratio of 1.05. Then, the sequentially rotated (SR) feeding scheme is utilized to construct a dual-port, dual-band, and dual-CP array with improved impedance and axial ratio (AR) bandwidth. For demonstration, a 2-by-2 subarray is constructed by two independent sets of sequentially feed network. Afterwards, an 8-by-8 array is proposed on the single-layer thin substrate. Finally, by utilizing the one-to-four power dividers and semirigid coaxial cables, a 16-by-16 array is successfully developed with high gain of more than 25 dBic. Measured results indicate that the two antenna arrays exhibit ideal radiation patterns and good isolations of better than 18 dB between two ports.

2. Design Concept

The specifications of the antenna to be designed are shown in Table 1. It is dual-port, dual-band, and orthogonal-CP at 8.2 and 8.6 GHz. The targeted gains of 25 dBic are not very high for single-band microstrip antenna arrays, which can be achieved with about 100 elements. However, they must be met for a dual-port shared-aperture array as well as specified frequencies and polarization. The bandwidths of 15 dB return loss (RL) and 3 dB axial ratio are 80 MHz in both bands. The fractional bandwidths are about 1%.

The frequency ratio is only 1.05. It is convenient to construct a shared-aperture array with equal element spacing in two bands, but it causes restrictions on the designs of the feed networks and shared-aperture elements (or subarray). For such a low frequency ratio, it is difficult to implement a diplexer with desirable isolations between two bands, so that two independent feed networks are required for dual-port designs. Shared-aperture elements (or subarray) can be designed with single-layer or multilayer configuration. For the former, four appropriate modes should be excited simultaneously in one patch to implement orthogonal-CP in dual bands; however, it is difficult for the frequency ratio of 1.05. For the latter, the overlapped patches on two layers are required, but strong coupling significantly increases the design complexity. Moreover, the fabrication of multilayer antennas is rather difficult and costly. Therefore, we choose to design with a single-layer configuration.

Table 1: Design parameters for dual port, dual-band, orthogonal-CP antenna.

Parameters	Receiving	Transmitting
Frequency (GHz)	8.2	8.6
Bandwidth (MHz)	80	80
Polarization	RHCP	LHCP
Return loss (dB)	≥15	≥15
Axial ratio (dB)	<3	<3
Gain (dBic)	>25	>25
Isolation (dB)	>20	>20

After a preliminary investigation, two candidates of the shared-aperture array on a single-layer substrate were investigated: (1) interlaced array consisting of two independent CP arrays in two bands; (2) shared-aperture array with sequential-rotated CP subarrays consisting of LP elements.

The first configuration is formed by using two independent interlaced arrays consisting of CP patch elements and feed networks. It is difficult to interlace two independent corporate-fed arrays with appropriate element spacing and without crossing in a single layer. Series-fed arrays are relatively easy; however, they suffer from very low bandwidth and tilted beam at frequencies off the center.

The second configuration of shared-aperture array adopts the sequentially rotated CP subarray as a unit cell. The SR technique was first proposed in [15], which substantially improves the bandwidth and polarization purity of CP arrays in spite of using the narrow band elements [16, 17]. Either LP or CP elements can be adopted to construct a SR array; however, LP rectangular patch has two orthogonal dominant modes which can realize dual-band radiation with very small frequency ratio as well as desired isolation. The following design is based on this configuration.

The patch with edges L_1 and L_2 of unequal length is adopted and shown in Figure 1. Two orthogonal dominant modes TM_{01} and TM_{10} are excited by two microstrip lines at the center of the orthogonal edges L_1 and L_2 for 8.2 and 8.6 GHz, respectively.

A basic SR subarray has its elements arranged in a 2-by-2 square or rectangular grid configuration with element angular orientation and feed phase arranged in either $0^\circ, 90^\circ, 0^\circ, 90^\circ$ or $0^\circ, 90^\circ, 180^\circ, 270^\circ$ fashion. In the latter arrangement, the axial ratio bandwidth of the array can be increased substantially [17]. Either parallel feed or serial feed can be used for a SR array [18]. Here, both of them are utilized to construct a dual-band dual-CP subarray with dual ports based on the dual-band dual-LP elements.

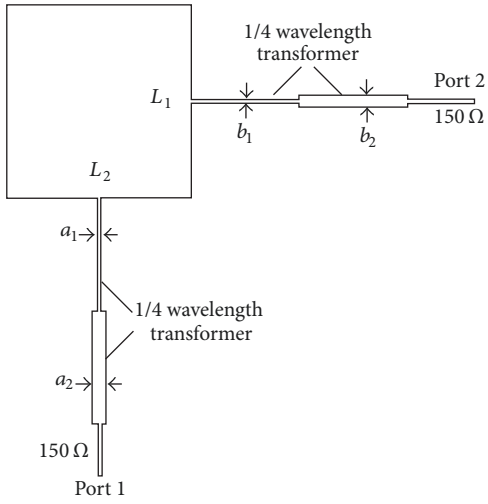

Figure 1: Structure of dual-band dual-LP element.

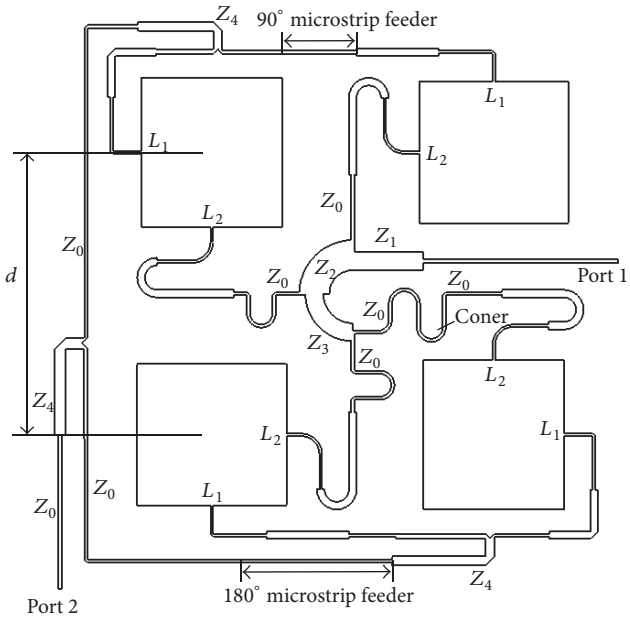

Figure 2: Structure of dual-band dual-CP subarray.

The 2-by-2 subarray is shown in Figure 2. Both the element angular orientation and feed phase are arranged in the 0°, 90°, 180°, 270° fashion. A serial feed network is placed at the array center and connected to L_2 to form right-hand circularly polarization (RHCP) for the lower band. Meanwhile, a parallel feed structure is placed outside the subarray and connected to L_1 to form left-hand circularly polarization (LHCP).

The proposed 2-by-2 subarray possesses all the desired features: being single-layer, dual-port, dual-band, dual-circular polarization and with a low frequency ratio. This subarray is taken as the unit cell to form an 8-by-8 array by using two independent sets of parallel feed networks. The cross-over of the feed lines in the two sets of the feed networks can be avoided through careful arrangement. By utilizing

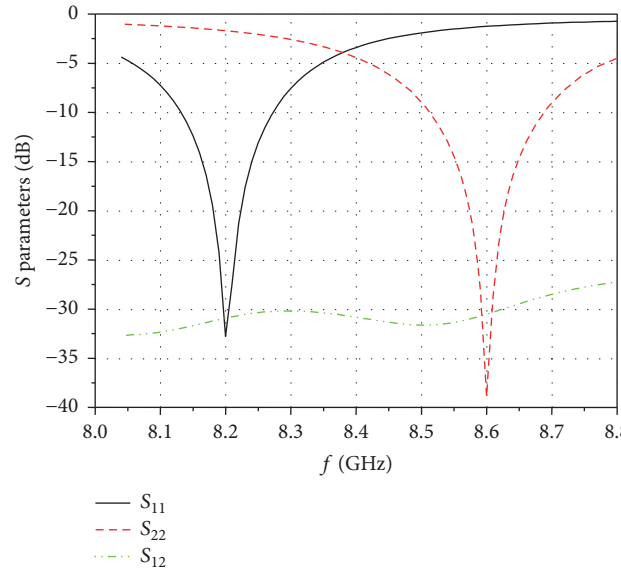

Figure 3: S parameters of the element.

one-to-four power dividers and semirigid coaxial cables, a 16-by-16 array is further developed. The performances of this design in various stages of development are provided below in detail.

3. Dual-Band Dual-LP Element

As illustrated in Figure 1, a dual-band dual-LP rectangular patch is designed on a single-layer substrate of Rogers RT/duroid 5880 with the relative permittivity of 2.2 and a thickness of 0.787 mm. The dimensions of edges L_1 and L_2 are 11.65 mm and 11.04 mm, corresponding to the frequencies f_1 = 8.2 GHz and f_2 = 8.6 GHz, respectively. Two orthogonal dominant modes TM_{01} and TM_{10} are excited by two microstrip lines at a pair of orthogonal edge-centers. In each feed line, a dual-section transformer consisting of two quarter-wavelength segments with impedance of 160 ohms and 100 ohms is introduced to match the patch to the feed line of 150 ohms. The line widths of the impedance transformers a_1, a_2, b_1, and b_2 are 0.2 mm, 0.8 mm, 0.2 mm, and 0.6 mm, respectively. Simulated S parameters of the element are shown in Figure 3. We can see that it matches well at two center frequencies, respectively. The corresponding 15 dB return loss bandwidths are 0.97% (8.16–8.24 GHz) and 1.05% (8.56–8.65 GHz). The isolations of two ports are better than 30 dB.

In this design, the frequency ratio is approximately equal to the ratio between the two orthogonal edges L_1 and L_2 of the patch. Because of the narrowband property and good polarization purity, two operating frequencies with a very low frequency ratio can be achieved with good isolations.

4. Dual-Band Dual-CP Subarray

4.1. Subarray Structure. As indicated in Figure 2, a 2-by-2 subarray is constructed by SR dual-band orthogonal-LP

Table 2: Impedance transformation values.

Feeder section	Z_0	Z_1	Z_2	Z_3	Z_4
Impedance values (Ω)	150	75	50	75	106

patches. All the elements match microstrip lines with characteristic impedance Z_0. The topological structure in Figure 2 is useful where dual-band, dual-port, and dual-circular polarization are required.

A serial feed network is placed at the array center and connected to L_2 to form RHCP for the lower band. It is modified from the one in Ref. [18]. The curved segments Z_2 and Z_3 perform as transitions rather than as quarter-wavelength impedance transformers. Only one-quarter-wavelength impedance transformer Z_1 is used to match the subarray to impedance Z_0. Therefore, the network can be more compact to be accommodated in an array with small element spacing. To meet the feed phase requirements, 90° phase shifts are achieved by stretching the length of corners along with the arcs.

A corporate network is placed outside the subarray and connected to L_1 to form LHCP. It is a combination of three 3 dB T-junction power dividers, in which a quarter-wavelength impedance transformer Z_4 is used. Impedance values of the transitions and impedance transformers are shown in Table 2, which ensure equal power required for each element. The 90° phase shifts are achieved by adding two 90° and one 180° microstrip segments.

4.2. Element Spacing Selection. For a conventional microstrip patch array, maximum directivity is obtained when the element spacing is in the range of 0.8–0.9λ_0, where λ_0 denotes the wavelength in free space [19]. However, for a SR CP array with LP elements, gain bandwidth broadens for reduced spacing [20]. Therefore, element spacing d of the proposed array should be chosen as small as possible. To accommodate the patch and feed networks, d is chosen as 22 mm, about 0.6λ_1 and 0.63λ_2, where λ_1 and λ_2 are the free space wavelengths of f_1 = 8.2 GHz and f_2 = 8.6 GHz, respectively.

4.3. Simulated Results. Simulated S parameters of the subarray are shown in Figure 4. It is seen that desired matching at two ports is obtained for both frequency bands. The 15 dB RL bandwidths are 3.92% (8.00–8.32 GHz) and 3.15% (8.43–8.7 GHz) in the lower and upper bands, respectively. The bandwidths are obviously broadened. The isolations between two ports are 20 dB and 16 dB at 8.2 GHz and 8.6 GHz, respectively. We can see that the isolation performance deteriorates obviously. This is the result of the broadening of the bandwidth and the coupling between the feeder and the patch. However, the insertion of a bandpass filter in an independent feed network can easily increase the isolation of up to 20 dB.

Simulated ARs versus frequency are shown in Figure 5. The 3 dB AR bandwidths are 3.23% (8.075–8.34 GHz) and 1.28% (8.57–8.68 GHz) in the lower and upper bands, respectively.

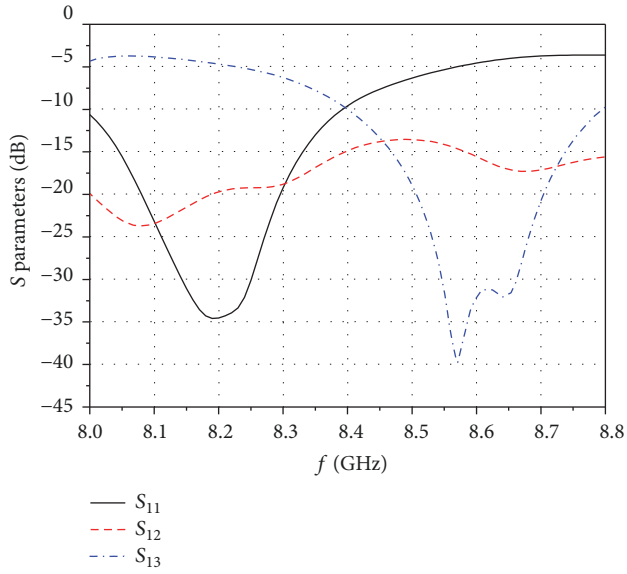

Figure 4: S parameters of the subarray.

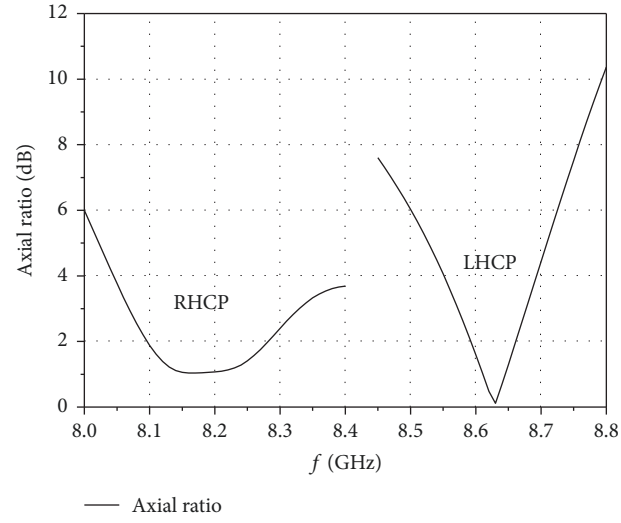

Figure 5: ARs of the subarray versus frequencies.

Gain patterns are shown in Figure 6. Maximum gains of 10.5 dBic and 11.29 dBic are obtained at 8.2 GHz and 8.6 GHz, respectively. It is seen that the patterns are much symmetrical and the cross polarization levels are below −20 dB in two principle planes. However, high cross-polarized lobes appear in the φ = 45° plane. The high diagonal lobes can be significantly reduced when the sequential array is placed in a larger array environment that will be shown in Section 5.

For SR arrays, the gain bandwidth is dependent on the elements' polarization properties. The array factor (AF) of the 4-element subarrays with different polarized elements is investigated in [21]. It shows that, for an SR array with LP elements, the AF is generally independent of frequency, but the maximum is 3 dB lower than an array with CP elements. That is the reason why the gains of the propose dual-band array are about 3 dB lower than those of a conventional

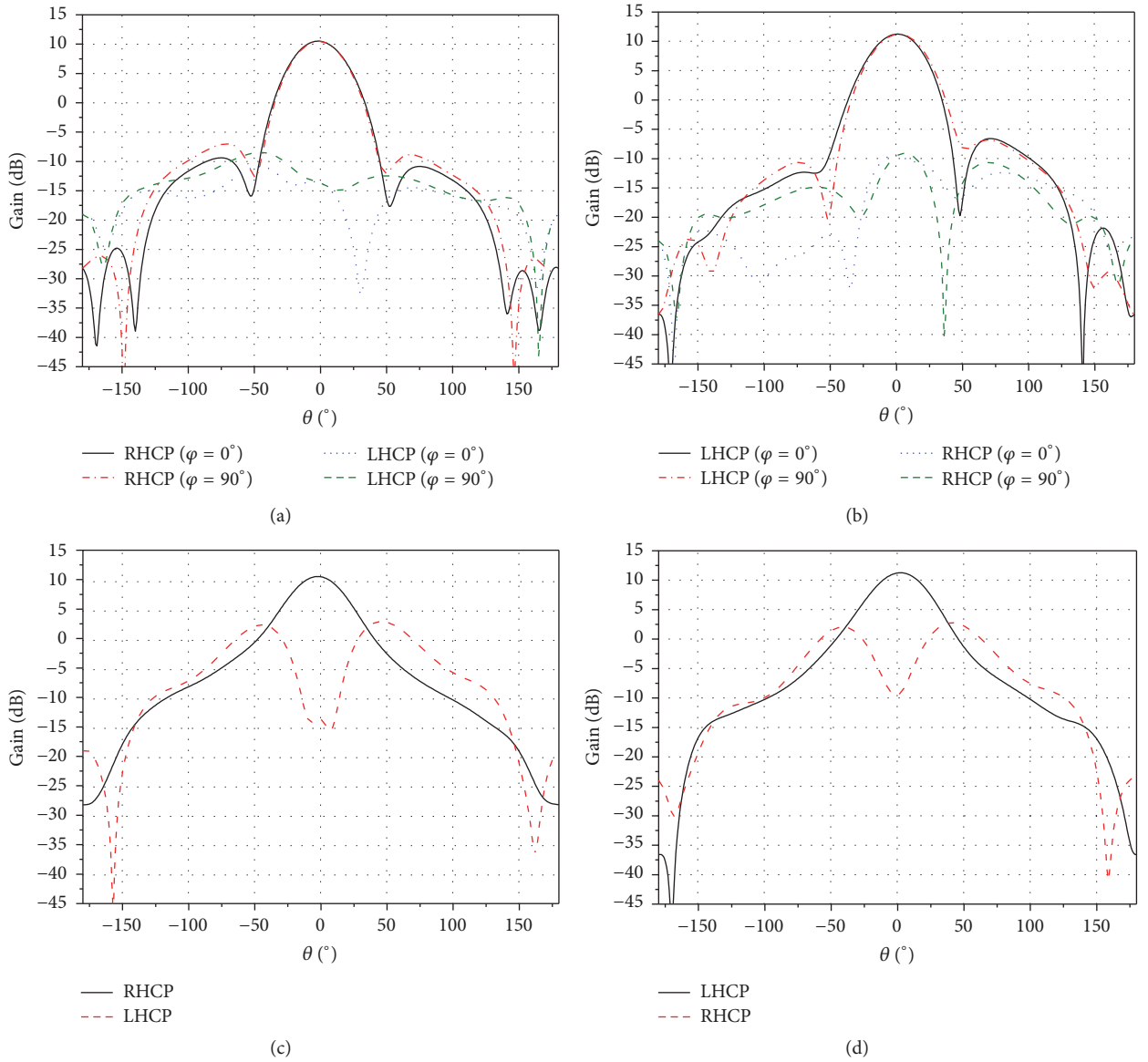

Figure 6: Gain patterns at two center frequencies: (a) gain patterns in two principle planes at 8.2 GHz; (b) gain patterns in two principle planes at 8.6 GHz; (c) gain patterns in the $\varphi = 45^\circ$ plane at 8.2 GHz; (d) gain patterns in the $\varphi = 45^\circ$ plane at 8.6 GHz.

4-element microstrip array, and the gain bandwidth is mainly determined by the minimum of the impedance and AR bandwidth.

5. 8-by-8 Dual-Band Dual-CP Array

5.1. 8-by-8 Array Structure. Considering the 2-by-2 subarray as a dual-port unit, an 8-by-8 array on a single-layer substrate is designed and fabricated. As shown in Figure 7, a hard plastic plate with a thickness of 4 mm is set on the back. Two independent sets of parallel feed networks are used to feed 16 subarrays. It is seen that the designed layout can avoid the cross-over of feed lines in the two sets of the feed networks.

To accommodate the networks and reduce the coupling between feed lines, the spacing is chosen as $d = 22$ mm, $d_1 = 28$ mm, $d_2 = 26$ mm, and $d_3 = 32$ mm. The feed networks should be adjusted carefully for appropriate amplitudes and phases. The array dimension is 220 mm × 220 mm.

Table 3: Optimized values of S parameters and ARs.

Port	S_{11} (dB)	S_{12} (dB)	S_{22} (dB)	AR (dB)
1@8.2 GHz	−18.8	−23.6	−9.0	1.67
2@8.6 GHz	−5.71	−20.2	−24.7	1.41

5.2. Simulated and Measured Results. S parameters and ARs are optimized at two center frequencies, and the optimal values are shown in Table 3. Good impedance matching, moderate isolations, and desired CP radiation are achieved

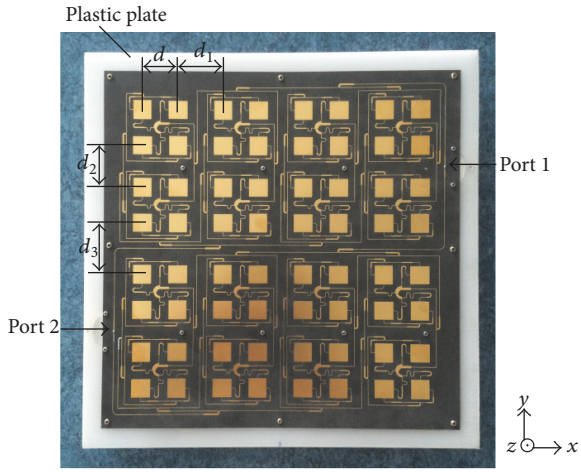

Figure 7: Photo of the fabricated antenna array.

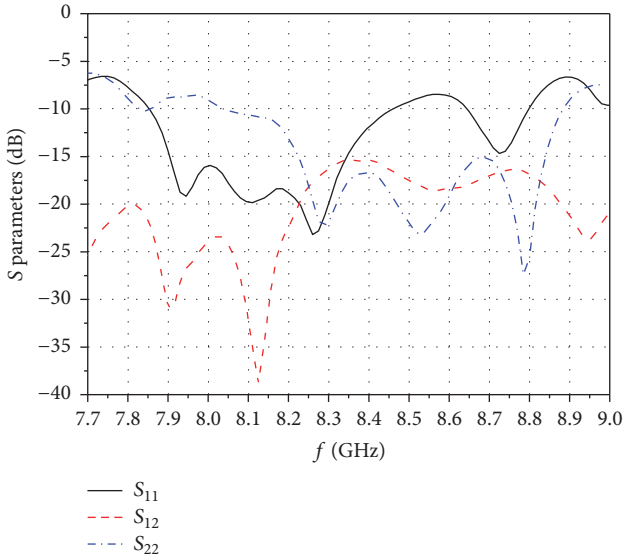

Figure 8: S parameters of the 8 by 8 array.

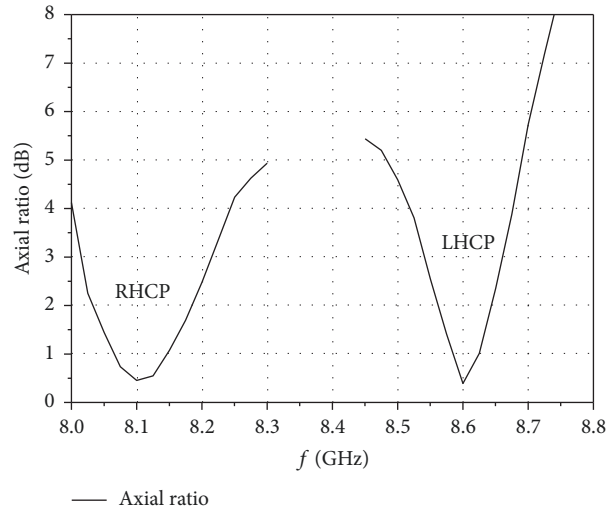

Figure 9: ARs of the 8-by-8 array versus frequencies.

simultaneously. Measured S parameters with desired performances are shown in Figure 8. The 15 dB RL bandwidths are 5.3% (7.91–8.34 GHz) and 7% (8.23–8.83 GHz) in the lower and upper bands, respectively. The isolations between two ports are 22.4 dB and 18.5 dB at 8.2 GHz and 8.6 GHz, respectively. We found that the impedance bandwidths are further broadened, which can be attributed to the increase of loss and coupling in the array. However, the isolations do not deteriorate further, even though two band overlap to some extent. It can be explained by the measured ARs shown in Figure 9. The 3 dB AR bandwidths are 3.23% (8.02–8.22 GHz) and 1.39% (8.54–8.66 GHz) in the lower and upper bands, respectively, which are close to those of the subarray. The minimum ARs of 0.45 dB and 0.4 dB are obtained, respectively, at 8.1 GHz and 8.6 GHz. This is ideal for CP performance to ensure good isolation. It is also found that the frequency deviation of the minimum AR is very small, which is due to the error in simulation and manufacturing process. At 8.2 GHz, the AR of 2.48 dB is acceptable.

Patterns at 8.1 GHz and 8.6 GHz are simulated and measured. Normalized patterns in the $\varphi = 0^\circ$ plane are shown in Figure 10. Measured and simulated results maintain good consistency. The patterns are very symmetric and have very low cross polarization level in the main beam. Half-power beamwidths of 9.1° and 8.8°, and side lobes of −11 dB and −10 dB are obtained at 8.1 GHz and 8.6 GHz, respectively. Normalized patterns in the $\varphi = 45^\circ$ plane at 8.1 GHz are also given in Figure 11. It can be seen that the cross polarization reduces to −11.3 dB and is far away from the main beam. This is because of the small spacing of the subarray and the averaging effects of the large array.

The measured gains of 20.1 dBic and 20.5 dBic are obtained at 8.2 GHz and 8.6 GHz, respectively. While simulated gains are 21.3 dBic and 21.9 dBic. The deviations are mainly attributed to the fabrication tolerances and the dielectric and conductive loss.

5.3. Discussion on Array Configuration. In the above discussion, two independent sets of parallel feed networks are used to extend the subarray to the 8-by-8 array. The SR feed networks can be adopted again to further broaden the 15 dB RL and 3 dB AR bandwidth [18]. In that case, however, the gain bandwidth will decrease. In addition, the complexity of array arrangement will also increase dramatically for the dual-band shared-aperture antenna array.

6. 16-by-16 Dual-Band Dual-CP Array

To achieve higher gains, a 16-by-16 array is designed. Because of the rapid increase of loss, microstrip line is not the advisable choice to expand the feed network. A one-to-four power divider (PD) and semirigid coaxial cables are used to set up the 16-by-16 array, which are shown in Figures 12 and 13, respectively. The PD consists of four symmetric quarter-wavelength impedance transformers to achieve complete

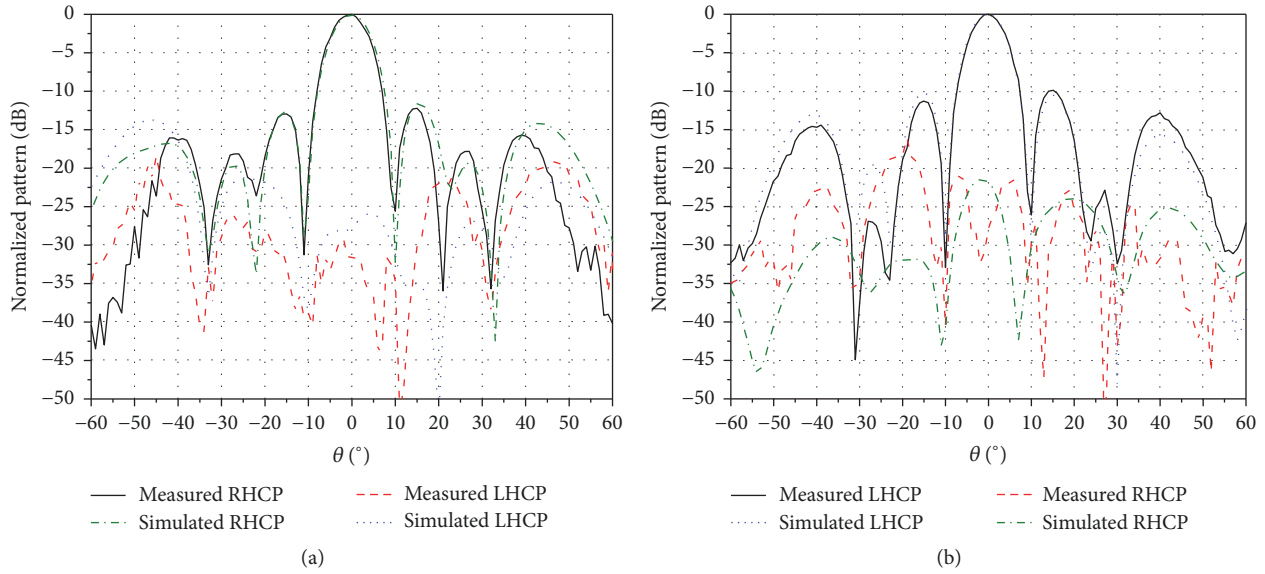

FIGURE 10: Normalized patterns in the $\varphi = 0^\circ$ plane: (a) 8.1 GHz; (b) 8.6 GHz.

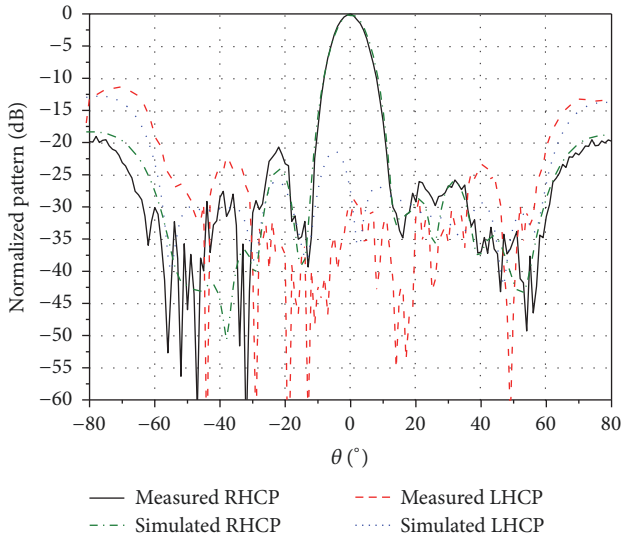

FIGURE 11: Normalized patterns in the $\varphi = 45^\circ$ plane at 8.1 GHz.

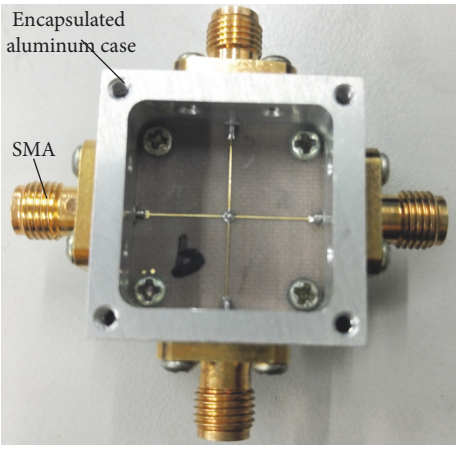

FIGURE 12: Photo of one-to-four power divider.

FIGURE 13: Photo of a semirigid coaxial cable.

impedance matching. Two independent PDs are designed for upper and lower bands, respectively. Measured return losses at the input ports are better than 20 dB over the operating bands. Insertion losses between input and output ports are less than 6.5 dB. Amplitude and phase deviations between four ways are less than 0.15 dB and 2°, respectively. The semirigid coaxial cables have a low insertion loss of about 0.1 dB and a small phase deviation less than 2°. Therefore, desired balance of amplitude and phase can be achieved. The total insertion loss, including the PD, the coaxial cables, and SMA connectors, is about 1 dB.

The fabricated 16-by-16 array is shown in Figure 14. It is seen from Figure 14(a) that the array consists of four 8-by-8 arrays with spacing values d_4 and d_5 of 32 mm, about $0.87\lambda_1$ and $0.92\lambda_2$. The array has a size of 424×424 mm^2 and is fixed on a hard plastic plate with a thickness of 4 mm. Figure 14(b) shows the connections between the 8-by-8 subarray ports connected by the one-to-four power dividers and semirigid coaxial cables.

Measured S parameters are shown in Figure 15. The impedance bandwidths are 4.81% (7.91–8.30 GHz) and 6.75% (8.30–8.88 GHz) for 15 dB RL in the lower and upper bands, respectively. At 8.2 GHz and 8.6 GHz, the isolations between

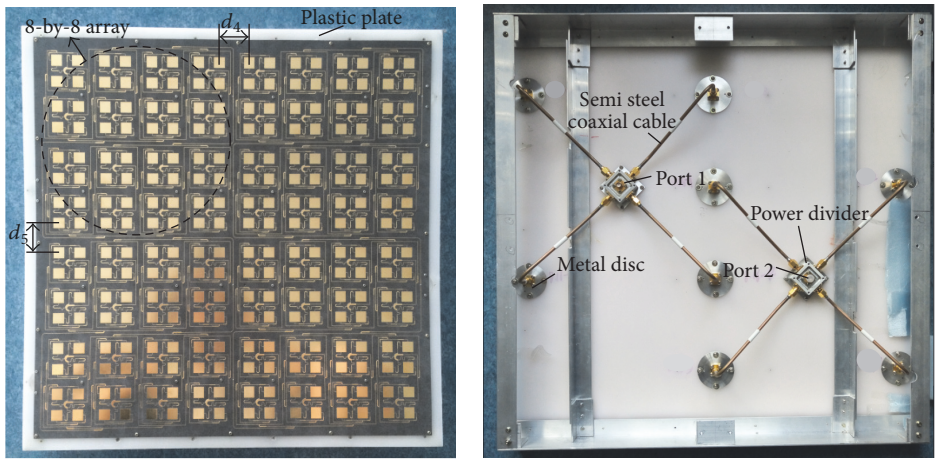

Figure 14: Photos of the fabricated 16-by-16 antenna array: (a) top view; (b) bottom view.

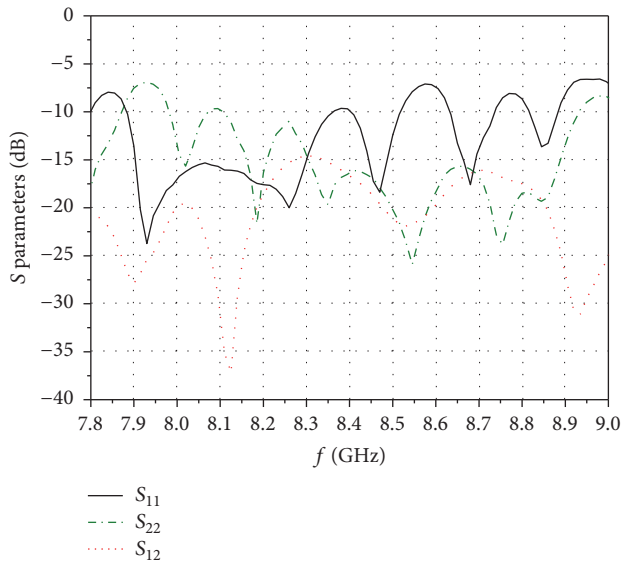

Figure 15: S parameters of the 16-by-16 array.

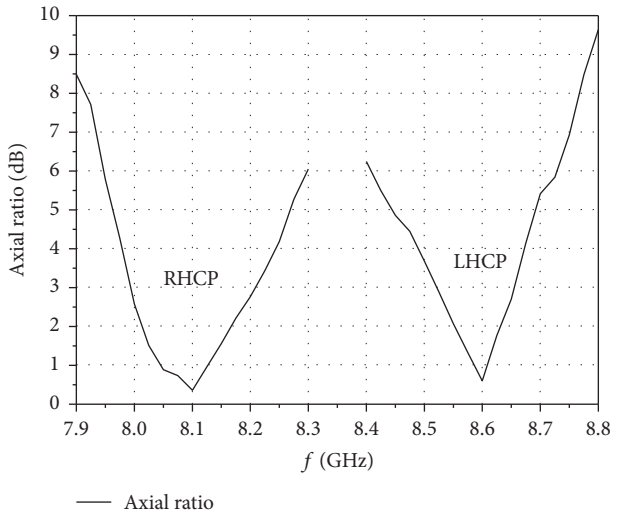

Figure 16: ARs of the 16-by-16 array versus frequencies.

two ports are 18.6 dB and 19.4 dB, respectively. Measured ARs are shown in Figure 16. The 3 dB AR bandwidths are 2.84% (7.99–8.22 GHz) and 1.57% (8.52–8.66 GHz) in the lower and upper bands, respectively, which are close to those of the subarray and the 8-by-8 array. Minimum ARs of 0.4 dB and 0.6 dB are obtained at 8.1 GHz and 8.6 GHz, respectively. The small deviation of the minimum AR frequency in the lower band is in accordance with the deviation of the 8-by-8 array. At 8.2 GHz, the AR of 2.8 dB is acceptable.

Patterns are measured at 8.1 GHz and 8.6 GHz. Normalized patterns in the $\varphi = 0^\circ$ plane are shown in Figure 17. The patterns are very symmetrical and have very low cross polarization levels in the main beam. Half-power beamwidths of 4.4° and 4.1°, and side lobes of −11.7 dB and −11 dB are obtained at 8.1 GHz and 8.6 GHz, respectively. Normalized patterns in the $\varphi = 45^\circ$ plane at 8.1 GHz are also given in Figure 18. It can be seen that the cross polarization level is decreased to −15.9 dB and far away from the main beam. This demonstrates that better cross polarization performance can be obtained for larger arrays.

Measured gains of 25.1 dBic and 25.6 dBic are obtained at 8.2 GHz and 8.6 GHz, respectively, which are in accordance with the measured results of the 8-by-8 array and the connection networks.

7. Conclusion

In this paper, a single-layer, dual-port, dual-band, and dual-CP microstrip antenna array is proposed. The frequencies of 8.2 GHz and 8.6 GHz with a ratio of 1.05 have been realized by adopting a dual-band orthogonal-LP rectangular patch as the elements. Two independent sets of SR feed networks are utilized to combine the dual-band, dual-LP elements into a

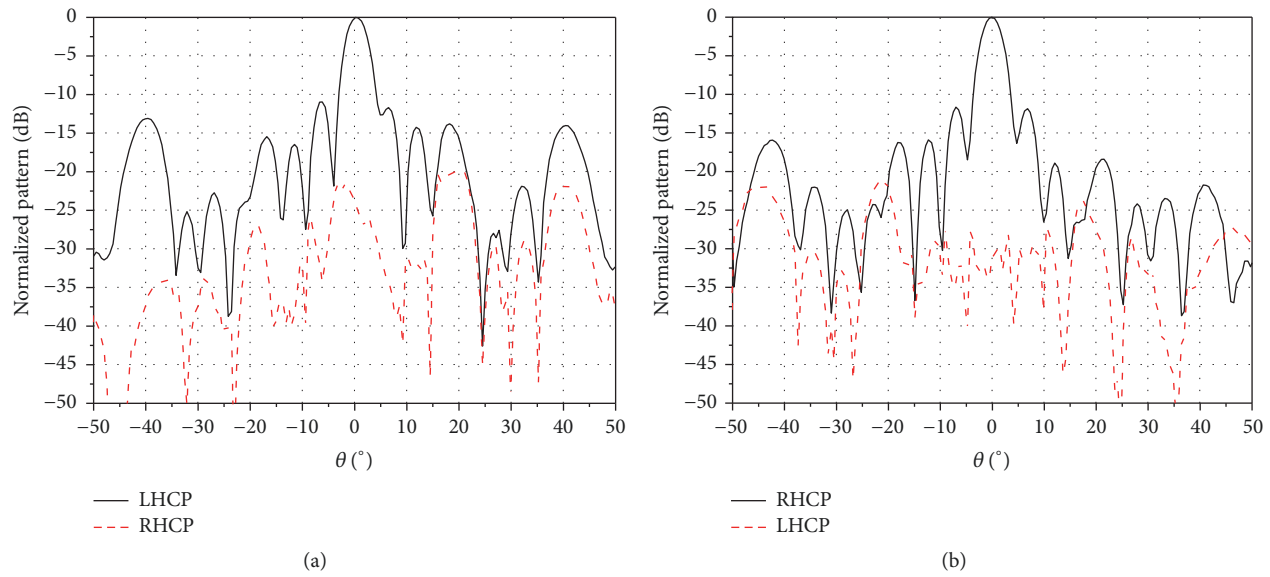

FIGURE 17: Measured normalized patterns in the $\varphi = 0^\circ$ plane: (a) normalized patterns in the $\varphi = 0^\circ$ plane at 8.1 GHz; (b) normalized patterns in the $\varphi = 0^\circ$ plane at 8.6 GHz.

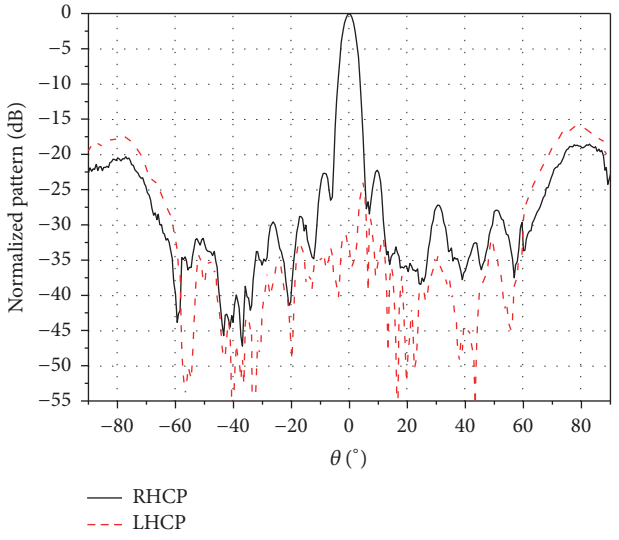

FIGURE 18: Measured normalized patterns in the $\varphi = 45^\circ$ plane.

2-by-2 dual-band, dual-CP subarray. This subarray is taken as the unit cell and the 8-by-8 array is successfully designed on the single-layer substrate. Furthermore, with the help of the one-to-four power dividers and semirigid coaxial cables, a 16-by-16 array is also developed to achieve higher gains. Measured results of the 8-by-8 and 16-by-16 arrays show that good CP performance, impedance, and AR bandwidths have been obtained. Measured gains more than 25 dBic have been achieved for the 16-by-16 array. Isolations between two ports can be improved up to 20 dB conveniently by inserting bandpass filters into the independent feed networks.

The proposed array has advantages of the single-layer and dual-port structure and dual-band dual-polarized performance. Therefore, it would be a good candidate for satellite communication systems, especially for dual-band applications with a very low frequency ratio.

Conflicts of Interest

The authors declare that they have no conflicts of interest.

Acknowledgments

The authors would like to acknowledge National Natural Science Foundation of China for funding this study under the General Program entitled "Pattern Synthesis on the Conical Beam Antennas for the Applications of Vehicle-Borne Satellite Communication and Missile-Borne Detection System" (Project Code 61771242).

References

[1] S. Du, Q.-X. Chu, and W. Liao, "Dual-band circularly polarized stacked square microstrip antenna with small frequency ratio," *Journal of Electromagnetic Waves and Applications*, vol. 24, no. 11-12, pp. 1599–1608, 2010.

[2] C.-X. Mao, S. Gao, Y. Wang, Q. Luo, and Q.-X. Chu, "A shared-aperture dual-band dual-polarized filtering-antenna-array with improved frequency response," *Institute of Electrical and Electronics Engineers. Transactions on Antennas and Propagation*, vol. 65, no. 4, pp. 1836–1844, 2017.

[3] S. Kumar, B. K. Kanaujia, M. K. Khandelwal, and A. K. Gautam, "Stacked dual-band circularly polarized microstrip antenna with small frequency ratio," *Microwave and Optical Technology Letters*, vol. 56, no. 8, pp. 1933–1937, 2014.

[4] K. Wincza and S. Gruszczynski, "Series-Fed Dual-Band Dual-Polarized Antenna Lattice Fed by Slot-Coupled Power Dividers," *IEEE Antennas and Wireless Propagation Letters*, vol. 15, pp. 1065–1068, 2016.

[5] M. Fakheri, M. Naser-Moghadasi, and R. A. Sadeghzadeh, "A broad band circularly polarized cross slot cavity back array antenna with sequentially rotated feed network for improving gain in X-band application," *International Journal of Microwave and Wireless Technologies*, pp. 1–6, 2016.

[6] X. L. Bao and M. J. Ammann, "Compact annular-ring embedded circular patch antenna with cross-slot ground plane for circular polarisation," *IEEE Electronics Letters*, vol. 42, no. 4, pp. 192-193, 2006.

[7] S. Feng, E. Nishiyama, and M. Aikawa, "Broad-band circularly polarized ring-slot array antenna for simultaneous use of the orthogonal polarizations," *IEICE Transactions on Electronics*, vol. E93-C, no. 7, pp. 1105–1110, 2010.

[8] Q. Zhang and W. Wu, "Dual-band microstrip-fed cavity-backed slot array of circular polarization," in *Proceedings of the IEEE Antennas and Propagation Society International Symposium (APSURSI '13)*, pp. 1720-1721, July 2013.

[9] M.-T. Tan and B.-Z. Wang, "A Dual-Band Circularly Polarized Planar Monopole Antenna for WLAN/Wi-Fi Applications," *IEEE Antennas and Wireless Propagation Letters*, vol. 15, pp. 670–673, 2016.

[10] D. Yu, S.-X. Gong, Y.-T. Wan, and W.-F. Chen, "Omnidirectional dual-band dual circularly polarized microstrip antenna Using TM_{01} and TM_{02} modes," *IEEE Antennas and Wireless Propagation Letters*, vol. 13, pp. 1104–1107, 2014.

[11] Z.-X. Liang, D.-C. Yang, X.-C. Wei, and E.-P. Li, "Dual-Band Dual Circularly Polarized Microstrip Antenna with Two Eccentric Rings and an Arc-Shaped Conducting Strip," *IEEE Antennas and Wireless Propagation Letters*, vol. 15, pp. 834–837, 2016.

[12] J.-D. Zhang, W. Wu, and D.-G. Fang, "Dual-band and dual-circularly polarized shared-aperture array antennas with single-layer substrate," *Institute of Electrical and Electronics Engineers. Transactions on Antennas and Propagation*, vol. 64, no. 1, pp. 109–116, 2016.

[13] J.-D. Zhang, L. Zhu, N.-W. Liu, and W. Wu, "Dual-band and dual-circularly polarized single-layer microstrip array based on multiresonant modes," *Institute of Electrical and Electronics Engineers. Transactions on Antennas and Propagation*, vol. 65, no. 3, pp. 1428–1433, 2017.

[14] M. Wang, W. Wu, and D.-G. Fang, "Uniplanar single corner-fed dual-band dual-polarization patch antenna array," *Progress in Electromagnetics Research Letters*, vol. 30, pp. 41–48, 2012.

[15] T. Teshirogi, M. Tanaka, and W. Chujo, "Wideband circularly polarised array antenna with sequential rotations and phase shift of elements," in *Proceedings of the in Proceedings ofIEEEInternational Symposium on Antennas and Propagation*, vol. 1, pp. 117–120, Tokyo, Japan, 1985.

[16] P. S. Hall, J. S. Dahele, and J. R. James, "Design principles of sequentially fed, wide bandwidth, circularly polarised microstrip antennas," *IEE Proceedings Part H Microwaves, Antennas and Propagation*, vol. 136, no. 5, pp. 381–389, 1989.

[17] P. S. Hall, J. Huang, E. Rammos, and A. Roederer, "Gain of circularly polarised arrays composed of linearly polarised elements," *IEEE Electronics Letters*, vol. 25, no. 2, pp. 124-125, 1989.

[18] M. N. Jazi and M. N. Azarmanesh, "Design and implementation of circularly polarised microstrip antenna array using a new serial feed sequentially rotated technique," *IEE Proceedings Microwaves, Antennas and Propagation*, vol. 153, no. 2, pp. 133–140, 2006.

[19] E. Levine, G. Malamud, S. Shtrikman, and D. Treves, "A Study of Microstrip Array Antennas with the Feed Network," *IEEE Transactions on Antennas and Propagation*, vol. 37, no. 4, pp. 426–434, 1989.

[20] P. S. Hall, "Application of sequential feeding to wide bandwidth, circularly polarised microstrip patch arrays," *IEE Proceedings Part H Microwaves, Antennas and Propagation*, vol. 136, no. 5, pp. 390–398, 1989.

[21] T. Zhang, W. Hong, and K. Wu, "Analysis and optimum design of sequential-rotation array for gain bandwidth enhancement," *Institute of Electrical and Electronics Engineers. Transactions on Antennas and Propagation*, vol. 63, no. 1, pp. 142–150, 2015.